Journal of Power Sources 196 (2011) 7169–7174

Contents lists available at ScienceDirect

Journal of Power Sources

journal homepage: www.elsevier.com/locate/jpowsour

Microstructural factors of electrodes affecting the performance of anode-supported thin film yttria-stabilized zirconia electrolyte (~1 μm) solid oxide fuel cells

Ho-Sung Noh[a,b], Heon Lee[b], Byung-Kook Kim[a], Hae-Weon Lee[a], Jong-Ho Lee[a], Ji-Won Son[a,*]

[a] High-Temperature Energy Materials Center, Korea Institute of Science and Technology, P.O. Box 131, Cheongryang, Seoul 130-650, Republic of Korea
[b] Dept. of Materials Science and Engineering, Korea University, Anam-dong, Seongbuk-Gu, Seoul 136-701, Republic of Korea

ARTICLE INFO

Article history:
Received 26 July 2010
Received in revised form
15 September 2010
Accepted 16 September 2010
Available online 22 September 2010

Keywords:
Thin film electrolyte solid oxide fuel cell
Yttria-stabilized zirconia
Pulsed laser deposition
Anode support
Cathode thickness

ABSTRACT

The effects of the microstructural factors of electrodes, such as the porosity and pore size of anode supports and the thickness of cathodes, on the performance of an anode-supported thin film solid oxide fuel cell (TF-SOFC) are investigated. The performance of the TF-SOFC with a 1 μm-thick yttria-stabilized zirconia (YSZ) electrolyte is significantly improved by employing anode supports with increased porosity and pore size. The maximum power density of the TF-SOFCs increases from 370 mW cm^{-2} to 624 mW cm^{-2} and then to over 900 mW cm^{-2} at 600 °C with increasing gas transport at the anode support. Thicker cathodes also improve cell performance by increasing the active reaction sites. The maximum power density of the cell increases from 624 mW cm^{-2} to over 830 mW cm^{-2} at 600 °C by changing the thickness of the lanthanum strontium cobaltite (LSC) cathode from 1 to 2–3 μm.

1. Introduction

Micro-solid oxide fuel cells (micro-SOFCs) have drawn much attention for their application as high performance portable and mobile power sources due to their advantages such as high energy density and fuel flexibility [1–5]. To realize miniaturized SOFC systems for portable applications, lowering the operating temperature without performance compromise should be accomplished for the thermal management, as well as for the reliability, of the integrated system by preventing chemical reaction between constituent material components [1–4]. One of the most attempted methods to lower the operating temperature of micro-SOFCs is employing thin film electrolytes. Thin electrolytes less than 1 μm were mostly realized in backside etched free-standing membrane designs [3–5]. However, due to the significant weakness in terms of thermal–mechanical stability of the thin membrane [6], it is desirable to fabricate a supported thin film electrolyte SOFC rather than a free-standing membrane SOFC. Nevertheless, it is highly challenging to obtain an appreciable OCV with a thin film electrolyte of a thickness less than a few microns over bulk ceramic processed substrates because of the surface roughness and porosity of the support [7–9].

In a previous study [1], a very uniform nano-structure anode interlayer with fine pores with sizes less than 200 nm was fabricated by using pulsed laser deposition (PLD). This layer worked as a surface modification layer of a tape-casted anode support [10]. On the basis of the nano-structure interlayer, an anode-supported thin film electrolyte SOFC (denoted as TF-SOFC hereafter) with a 1 μm-thick yttria-stabilized zirconia (YSZ) electrolyte was fabricated and it exhibited an open circuit voltage (OCV) value of over 1 V. The cell with a thin film electrolyte and nano-structure electrodes exhibited higher cell performances especially at low operating temperatures (350–550 °C) compared with those of thick film electrolyte SOFCs [1].

Despite the performance improvement with the thin electrolyte, the degree of performance increment was rather lower than expected. The TF-SOFC exhibited a lower power density than that of the bulk-processed 8 μm-thick film electrolyte SOFC at 600 °C [1]. There are two factors postulated to induce the performance compromise of the TF-SOFC. The first factor is the gas transport at the anode support. In Fig. 1(a), the AC impedance spectrum of the TF-SOFC at 600 °C is provided, and it is observable that the arc which appears at a low frequency range ($f \leq 1$ Hz) is pronounced [1]. The low frequency arc is known to be related to the mass transport

* Corresponding author. Tel.: +82 2 958 5530; fax: +82 2 958 5529.
E-mail address: jwson@kist.re.kr (J.-W. Son).

0378-7753/$ – see front matter © 2010 Elsevier B.V. All rights reserved.
doi:10.1016/j.jpowsour.2010.09.038

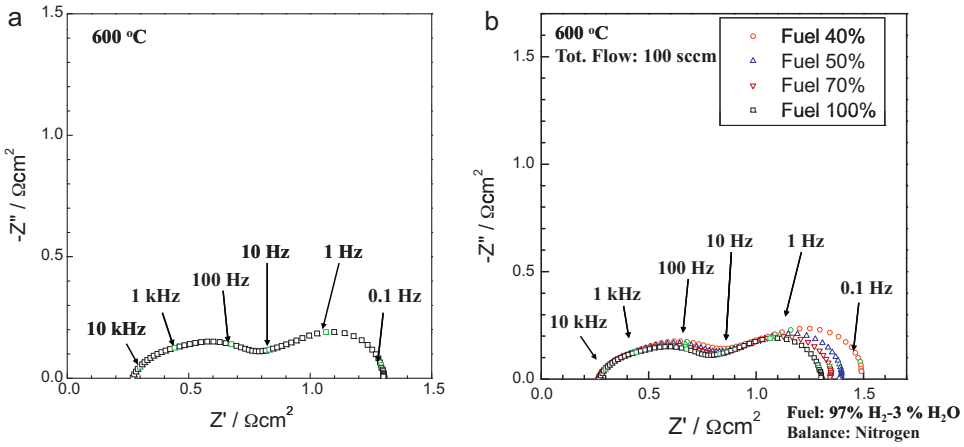

Fig. 1. (a) Impedance spectrum of TF-SOFC on tape-casted anode [1], and (b) impedance spectra of the same cell with the fuel partial pressure change.

[11]. When the partial pressure of the fuel at the anode side was varied, the low frequency arc changed with respect to the fuel partial pressure (Fig. 1(b)), which supports that the arc corresponds to the mass transport of the anode [12]. The effect of the concentration polarization at the anode is more significant than that in the cathode of the anode-supported cell due to the anode thickness, and the fuel partial pressure change strongly affects the concentration polarization [12,13]. In the *I–V* curves of the TF-SOFC, the concentration polarization was very significant at 550 and 600 °C [1], which is consistent with the observation in the impedance spectrum. Recently, it was reported that the microstructural difference of the anode can cause a significant performance change [12]. Thus, it is possible that the influence of the anode support microstructure on cell performance is not negligible at the low temperature regime. Therefore, the anode microstructure related to the mass transport, such as porosity and pore size, should be improved for fully taking advantage of the thin electrolyte in the anode-supported TF-SOFC.

The second factor is the limited active reaction sites of the cathode. Thinning down the electrodes would decrease the triple phase boundary (TPB) length, which would lead to performance reduction [14]. Therefore, using the thin film technology for fabricating the electrode is not as advantageous as in the electrolyte fabrication. The TF-SOFC reported [1] had a 1 μm-thick lanthanum strontium cobaltite (LSC) cathode, which might be insufficient for a satisfactory cell performance.

Therefore, in this report, we investigated the cell performance improvement of the TF-SOFC cell by changing the parameters such as the pore structure of the anode support and the thickness of the cathode. The tape-casted anode support properties were modified by changing the amount of the plasticizer. In addition, a comparison with a TF-SOFC formed on an anode support, fabricated by compaction molding with a screen printed anode functional layer (denoted as a C-SP anode support), which was proven to be the effective anode in the cells fabricated by powder process-

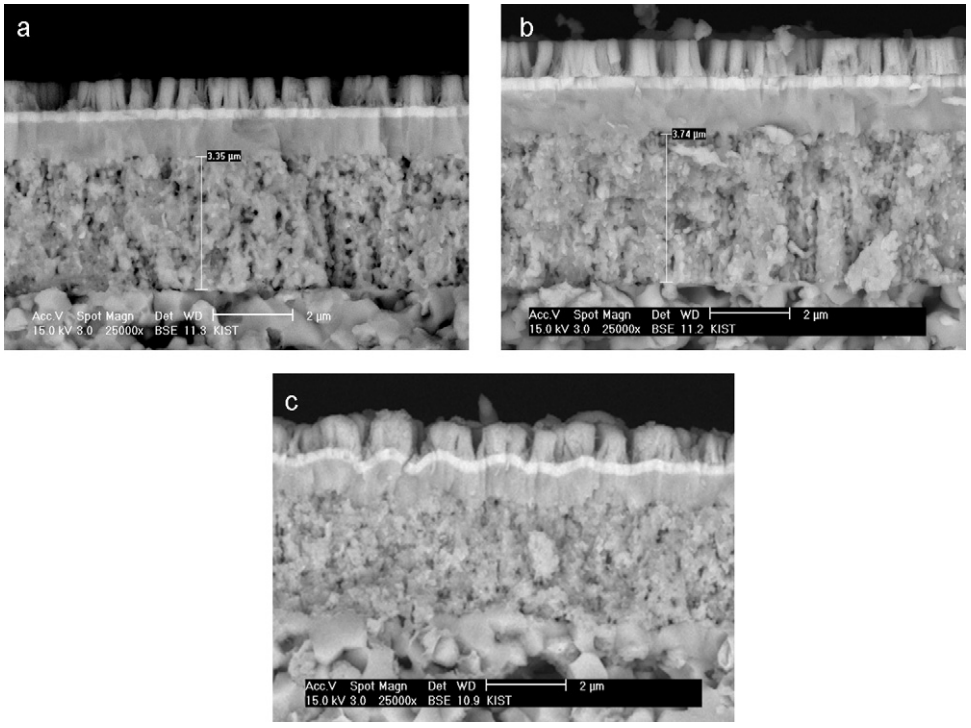

Fig. 2. Cross-sectional SEM-micrographs of TF-SOFCs on (a) T1, (b) T2, and (c) C-SP anode supports.

ing [15–17], was performed. The cathode thickness was varied by simply doubling or tripling the deposition duration. The *I–V* characteristics, impedance spectra (IS), and physical properties are correlated to elucidate the origin of the performance changes.

2. Experimental

2.1. Fabrication of TF-SOFC on various anode support types

The first generation tape-casted anode which was used in the previous report [1] (denoted as T1) was fabricated as follows: 112 g NiO and 88 g YSZ (NiO:8YSZ = 56:44 wt%, final Ni vol% in the solid content after reduction is 40 vol%) powders were dispersed in a 88 g ethanol and toluene mixture solvent to make the tape slurry. 2.6 g of a polymeric surfactant (Hypermer KD-1, Uniquema) and 16 g of polyvinylbutyral79 (PVB79) were added as a dispersant and a binder, respectively. 16 g of dibutylphthalate (DBP) was added as the plasticizer. Tapes with a thickness approximately 300 μm were fabricated by tape casting and three layers of tapes were laminated at 75 °C under a uniaxial pressure of 12.25 MPa. The sintering of T1 was performed at 1300 °C for 4 h in air.

The second generation tape anode (denoted as T2) was fabricated based on the same composition, except for the amount of DBP. DBP was increased from 16 g to 20 g to reduce the lamination defect and to improve the particle arrangement and packing during the lamination. Sintering and lamination conditions were identical with T1.

The C-SP anode support was fabricated as the following: NiO–YSZ (NiO:8YSZ = 56:44 wt%, final Ni vol% in the solid content after reduction is 40 vol%) composite powder granules were uni-axially warm pressed to form a green substrate body and an NiO–YSZ functional layer was screen printed over it [15–17]. The bi-layer anode support was sintered at 1400 °C for 3 h in air.

A 4 μm thick NiO–8YSZ nano-structure interlayer, a 1 μm-thick 8YSZ electrolyte, a 200 nm-thick gadolinia doped ceria ($Gd_{0.1}Ce_{0.9}O_{1.95}$, 10GDC) buffer layer, and a 1 μm-thick LSC

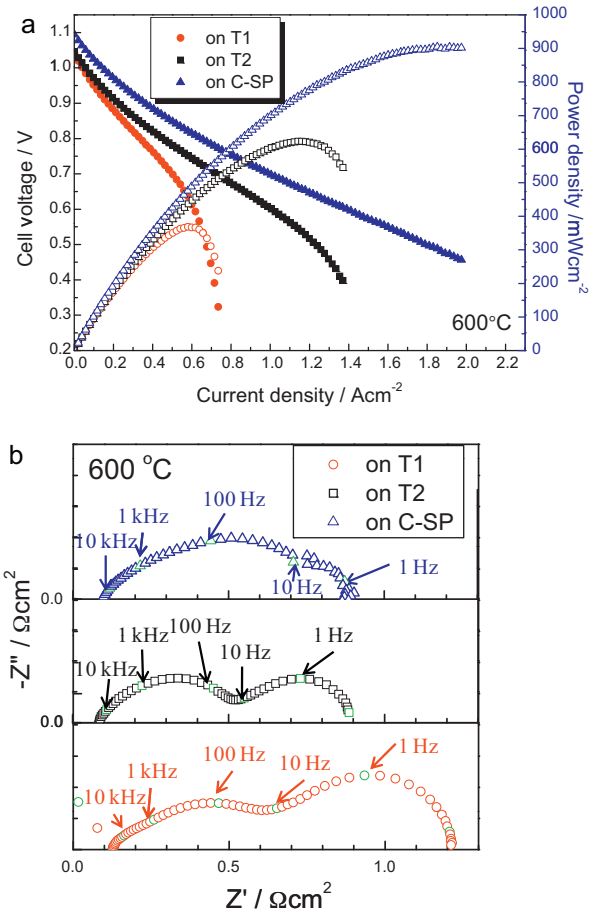

Fig. 3. (a) *I–V* curves and (b) ISs of TF-SOFCs on T1, T2, and C-SP anode supports.

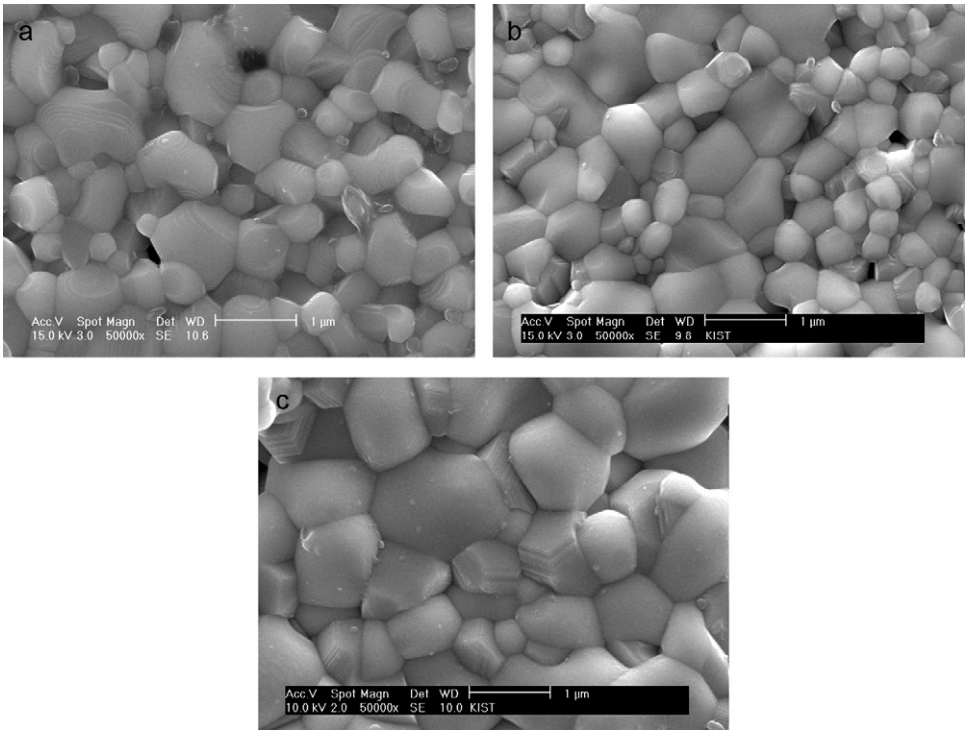

Fig. 4. Surface morphologies of (a) T1, (b) T2, and (c) C-SP anode supports.

($La_{0.6}Sr_{0.4}CoO_{3-\delta}$) cathode were fabricated using PLD on three different types of anode supports. A detailed fabrication scheme for the thin film components on the anode supports was reported elsewhere [1].

2.2. Fabrication of TF-SOFC with various cathode thicknesses

The T2 support was used for this series. 4 μm-thick NiO–YSZ nano-structure interlayer, 1 μm-thick YSZ electrolyte, and 200 nm-thick GDC buffer were fabricated over the T2 support. The LSC thickness was varied as 1, 2, and 3 μm. Cathode layers thicker than 3 μm had a delamination issue so the tested cathode thickness was controlled to be 1–3 μm.

2.3. Characterization of TF-SOFCs

The porosity and pore size distribution of the anode supports were analyzed by a mercury porosimeter (AutoPore IV 9510, Micromeritics). Microstructures were observed by using a scanning electron microscopy (SEM, XL-30 FEG, FEI). Electrochemical properties of the TF-SOFCs were measured by using a Solartron impedance analyzer with an electrochemical interface (SI1260 and SI1287, Solartron). The data measured at 600 °C are compared in this study to exclude the effect of the sealing consistency issue at lower temperatures [1].

Air and 97% H_2–3% H_2O were supplied as the oxidant and the fuel, respectively, and the gas flows were 200 sccm at both anode and cathode sides when *I–V* curves were measured.

3. Results and discussion

3.1. Cell performances of TF-SOFC on various anode supports

In Fig. 2, the cross-sectional microstructures of TF-SOFCs fabricated on T1, T2, and C-SP anodes are shown. The dimensions of each thin film component (interlayer, electrolyte, buffer, and cathode) are comparable in three cells. Due to the original surface roughness of the support, the undulation of the thin film components in the TF-SOFC on C-SP shown in Fig. 2(c) is more pronounced than that of the TF-SOFC on tape anodes shown in Fig. 2(a) and (b). Other than that, it is observed that the cells exhibit similar cross-sectional microstructures.

In Fig. 3(a), the *I–V* curves and power densities of the TF-SOFCs on T1, T2, and C-SP anodes measured at 600 °C are compared. For several repetitive measurements, all three cell types exhibited OCV values ranging from 1.0 to 1.1 V, which indicates that the thin electrolyte sustained microstructural integrity. However, the *I–V* characteristics are significantly different for the three cells. The TF-SOFC on T1 exhibited a substantial concentration polarization, thus the peak power density did not exceed ~400 mW cm^{-2} (370 mW cm^{-2}). The TF-SOFC on T2 showed a much reduced concentration polarization and the peak power density reached ~624 mW cm^{-2}. In the TF-SOFC on C-SP, concentration polarization was not observed and the peak power density reached over 900 mW cm^{-2}.

In Fig. 3(b), the IS of the three cells are presented. All cells had similar ohmic area specific resistance (ASR) of ~0.1 Ω cm^2, but the polarization ASRs were quite different. First, upon the change from T1 to T2, it is noticeable that the low frequency arc (frequency ~ 1 Hz) was reduced significantly. Second, upon the change from tape anodes (T1 and T2) to C-SP, the shape of the impedance spectra changed drastically. The low frequency arc of the TF-SOFC on C-SP was remarkably smaller than those of the TF-SOFC on tape anodes. As mentioned previously, the low frequency arc is affected by the gas diffusion of the electrode, especially the anode in anode-supported cells [12,13]. Both the *I–V* and IS indicate that the concentration polarization at the fuel side was improved from T1 to T2, and tape anodes to the C-SP anode.

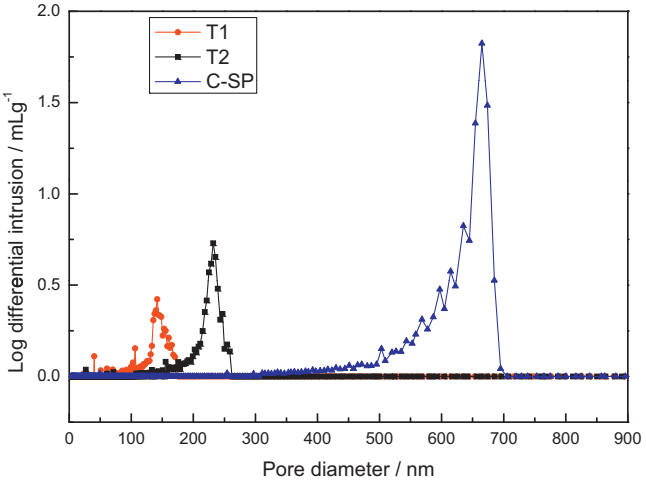

Fig. 5. Pore size distribution of T1, T2, and C-SP anode support after reduction.

Since the film components produced by thin film processing (PLD in this case) are very reproducible, the possible cause of the cell performance difference can be correlated to the microstructures of each anode support. In Fig. 4, the surface morphology of T1, T2, and C-SP anode supports are displayed. Tape anodes had a homogeneous fine porous structure throughout the whole thickness and the average grain size of tape anodes was ~0.53 ± 0.19 μm. The C-SP anode support consisted of the coarse porous support (~1 mm thick, average grain size ~0.96 ± 0.24 μm) fabricated by warm pressing and the fine porous structure anode functional layer (~15 μm thick, average grain size ~0.88 ± 0.16 μm) fabricated by screen printing. The grain size difference between the tape anode and the C-SP anode is postulated to be a reason of the improved gas transport in the C-SP anode. However, the difference between the T1 and T2 anodes could not be discerned by the images of the microstructures.

Therefore, for in-depth analysis of the pore structure of the anodes, mercury porosimetry was employed. In Fig. 5, the pore size distribution of T1, T2, and C-SP anodes after reduction are compared. The *y*-axis is mercury volume intruded per the sample mass, which corresponds to the pore volume of the samples. It is shown that T2 had a larger pore diameter and total pore volume than T1. The average pore size of T1 was 127.4 nm and that of T2 was 195 nm. Also, the porosity of T2 (~23%) was about 4% higher than that of T1 (~18.7%). The C-SP anode contained substantially larger pores and high porosity (average pore size ~ 542 nm, porosity ~ 34%) than tape-casted anodes. The difference between T1 and T2 explains the concentration polarization difference between the TF-SOFCs on those anode supports. The characteristic of the C-SP anodes provides a possible reason why there is almost no concentration polarization in the TF-SOFC on the C-SP support. The result provides pore-related physical properties of the anode types that can be correlated to the electrochemical performance differences. In addition, it indicates that the limitation of the gas transport from the porous support should be optimized to fully utilize the potential of the thin film electrolyte in the supported TF-SOFC design.

3.2. Cell performances of TF-SOFC with various cathode thicknesses

For investigating the effect of the cathode thickness, TF-SOFCs on the T2 support were selected for comparison. Although the TF-SOFC on the C-SP anode showed the best performance in the

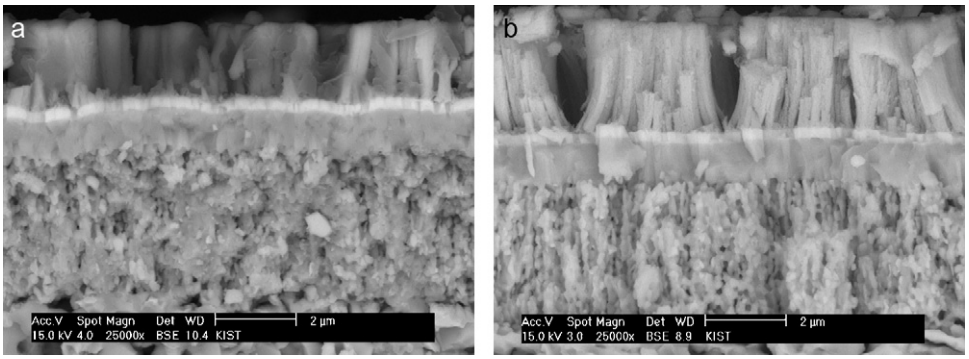

Fig. 6. Cross-sectional micrographs of (a) 2LSC, and (b) 3LSC cells.

previous section, the tape anode yielded a more consistent cathode microstructure due to less surface undulation. Thus, it was thought to be more appropriate to use the tape-casted anode for the experiments on the cathode. TF-SOFC cell with 1, 2, and 3 μm thick LSC cathode layers are denoted as 1LSC, 2LSC, and 3LSC, respectively. In Fig. 6(a) and (b), the cross-sectional microstructures of 2LSC and 3LSC are shown. The microstructure of 1LSC is shown in Fig. 2(b). The intended thickness difference of LSC cathodes was obtained and other thin film components were almost identical in dimension.

In Fig. 7(a), the *I–V* curves and power densities of 1LSC, 2LSC, and 3LSC are compared. In the *I–V* curves, the slopes of the *I–V* curves at the linear regime of 2LSC and 3LSC were smaller than that of 1LSC, i.e., the cell ASRs of 2LSC and 3LSC were decreased compared with that of 1LSC. 2LSC and 3LSC showed similar cell performances in which the peak power density was ~830 mW cm^{-2}. That of 1LSC was 624 mW cm^{-2}, as mentioned in the previous section.

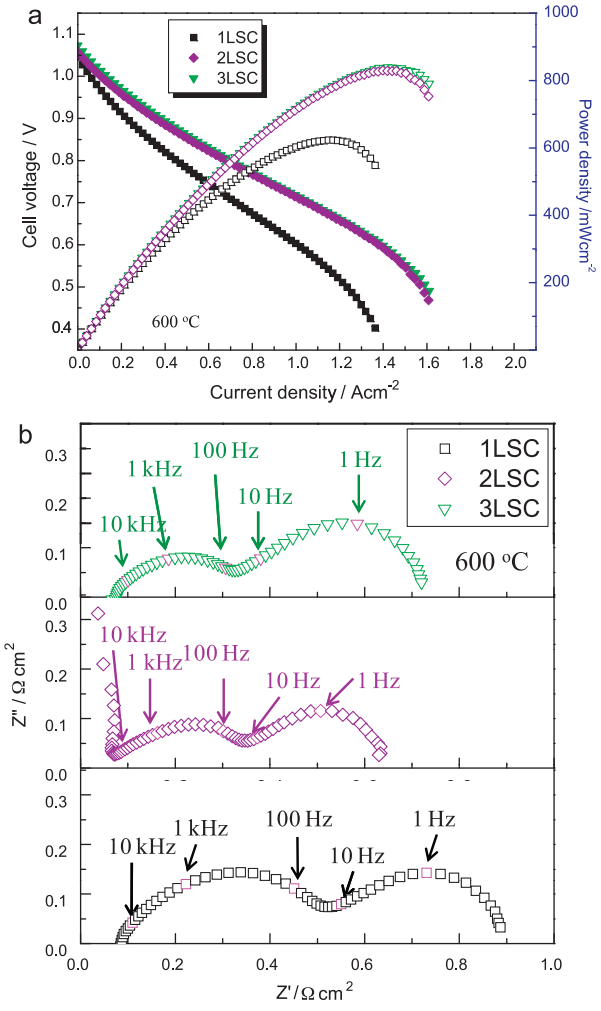

Fig. 7. (a) *I–V* curves and (b) ISs of 1LSC, 2LSC, and 3LSC cells.

In Fig. 7(b), the ISs at OCV of each cell are compared. All three cells again exhibited similar ohmic ASRs, about 0.1 Ω cm^2. There were differences in the exact size of the low frequency arcs, but the most noticeable difference was between 1LSC and others was the size of the arc appearing at a frequency higher than 10 Hz. When the concentration of the air side was varied, the size of the arc at $f \geq 10$ Hz was affected. Thus, it seems that the arc is indicative of the cathodic reaction, and it appears that the TF-SOFCs with thicker cathodes exhibit less polarization related to the cathode. Since LSC is a mixed ionic–electronic conductor (MIEC), the TPB zone is broadened to the entire surface of the cathode [14]. As the cathode thickens, the surface of the cathode increases and so does the number of the active reaction sites. Therefore, this leads to performance improvement of the TF-SOFC cells.

It cannot be definitely concluded that the effect of the thicker cathode saturates after 2 μm because it is possible that there is an additional effect from the gas transport of the anode support, especially seeing the size of the low frequency arc. However, in the given *I–V* curves, a similar trend in terms of the concentration polarization of three cells was observed, which implies that the effect of the gas transport was similar for three cells. Therefore, we postulate that 2–3 μm thick LSC can provide much less limited cell performance by the cathode thickness compared to 1 μm-thick LSC.

4. Conclusions

Microstructural parameters of electrodes affecting the cell performance of the anode-supported TF-SOFCs have been investigated. The limited performance of the TF-SOFC reported previously [1] appears to be mainly caused by the poor gas transport at the anode support. By changing the process for the support for improving the gas transport by changing the pore size and distribution, the cell performance of TF-SOFCs increased substantially. Cell performances were improved by 1.7–2.4 times from that of the TF-SOFC on the anode support with limited gas transport. This result shows that the limitation of the gas transport from the porous support should be optimized to fully utilize the potential of the thin film electrolyte in the supported TF-SOFC design.

The effect of the number of reaction sites at the thin film cathode was also studied. By increasing the thin film cathode thickness from 1 μm to 2–3 μm, the polarization from the cathodic reaction and cell ARS decreased significantly. By increasing the thickness of the cathode, cell performance improved by approximately 1.33 times. Based on these results, we expect to obtain high performance TF-

SOFCs, fully taking advantage of the thin electrolyte by controlling the pore structure of the anode supports and the thickness of the cathode.

Acknowledgement

This work was supported by the Institutional Research Program of Korea Institute of Science and Technology (KIST).

References

[1] H. Noh, J. Son, H. Lee, H. Song, H. Lee, J. Lee, J. Electrochem. Soc. 156 (2009) B1484–B1490.
[2] H. Noh, J. Park, J. Son, H. Lee, J. Lee, H. Lee, J. Am. Ceram. Soc. 92 (2009) 3059–3064.
[3] A. Evans, A. Bieberle-Hutter, J.L.M. Rupp, L.J. Gauckler, J. Power Sources 194 (2009) 119–129.
[4] A. Bieberle-Hutter, D. Beckel, A. Infortuna, U.P. Muecke, J.L.M. Rupp, L.J. Gauckler, S. Rey-Mermet, P. Muralt, N.R. Bieri, N. Hotz, M.J. Stutz, D. Poulikakos, P. Heeb, P. Muller, A. Bernard, R. Gmur, T. Hocker, J. Power Sources 177 (2008) 123–130.
[5] P.C. Su, C.C. Chao, J.H. Shim, R. Fasching, F.B. Prinz, Nano Lett. 8 (2008) 2289–2292.
[6] C.D. Baertsch, K.F. Jensen, J.L. Hertz, H.L. Tuller, S.T. Vengallatore, S.M. Spearing, M.A. Schmidt, J. Mater. Res. 19 (2004) 2604–2615.
[7] T. Ishihara, H. Eto, J. Yan, Int. J. Hydrogen Energy (2010), doi:10.1016/j.ijhydene.2009.1012.1174.
[8] B Hobein, F. Tietz, D. Stover, M. Cekada, P. Panjan, J. Eur. Ceram. Soc. 21 (2001) 1843–1846.
[9] T. Tsai, S.A. Barnett, J. Electrochem. Soc. 142 (1995) 3084–3087.
[10] H. Noh, J. Son, H. Lee, H. Ji, J. Lee, H. Lee, J. Eur. Ceram. Soc. 30 (2010) 3415–3426.
[11] T. Tsai, S.A. Barnett, J. Vac. Sci. Technol. A 13 (1995) 1073–1077.
[12] T. Suzuki, Z. Hasan, Y. Funahashi, T. Yamaguchi, Y. Fujishiro, M. Awano, Science 325 (2009) 852–855.
[13] S.H. Chan, K.A. Khor, Z.T. Xia, J. Power Sources 93 (2001) 130–140.
[14] S.J. Litzelman, J.L. Hertz, W. Jung, H.L. Tuller, Fuel Cells 8 (2008) 294–302.
[15] H. Jung, S. Choi, H. Kim, J. Son, J. Kim, H. Lee, J. Lee, J. Power Sources 159 (2006) 478–483.
[16] H. Jung, K. Hong, H. Jung, H. Kim, H. Kim, J. Son, J. Kim, H. Lee, J. Lee, J. Electrochem. Soc. 154 (2007) B480–B485.
[17] H. Jung, Y. Sun, H. Jung, J. Park, H. Kim, G. Kim, H. Lee, J. Lee, Solid State Ionics 179 (2008) 1535–1539.